Contribution from the Departments of Chemistry, University of California, Berkeley, California 94720, and University of Vermont, Burlington, Vermont 05405

X-ray Crystallographic Characterization of a Stepwise, Metal-Assisted Oxidative Decarboxylation: Vanadium Complexes of Ethylenebis[(*o*-hydroxyphenyl)glycine] and Derivatives

Paul E. Riley,[1] Vincent L. Pecoraro,[1] Carl J. Carrano,*[2] Joseph A. Bonadies,[2] and Kenneth N. Raymond*[1]

Received March 25, 1985

Vanadyl complexes of the synthetic ligand ethylenebis[(*o*-hydroxyphenyl)glycine] (EHPG) and a derivative have been prepared to elucidate the entities involved in a stepwise, metal-assisted oxidative decarboxylation to form VO(SALEN). The EHPG molecule contains two phenolate oxygens, two nitrogens, and two carboxylate oxygen ligating atoms and is thus a hexadentate ligand when fully deprotonated to the tetraanion. Treatment of a basic aqueous solution of EHPG with $VOSO_4 \cdot 3H_2O$ afforded light blue salt **1**, which was found by X-ray crystallography to be a distorted octahedral vanadyl complex, in which the EHPG ligand acts as a pentadentate donor with one of the two phenolate moieties remaining protonated and uncoordinated. In contrast, the reaction between $VOSO_4 \cdot 3H_2O$ and EHPG in aqueous ethanol yields a dark blue complex, which has been shown by a variety of spectroscopic techniques to be the neutral vanadium(V) complex in which the EHPG molecule again acts as a pentadentate ligand with a charge of 3-, but in comparison to **1**, we propose that a carbonyl group rather than a phenol group remains protonated and uncoordinated. This material is stable as a solid but decomposes in DMF solution to a green complex, which has been shown by X-ray crystallography to be VO(SALEN) (**3**), in which SALEN represents *N,N'*-disalicylideneethylenediamine. This reaction corresponds to an oxidative decarboxylation in which two molecules of CO_2, three protons, and three electrons are lost per VO(EHPG) complex in its transformation to the tetradentate VO(SALEN) complex. Evidence for the stepwise oxidative decarboxylation that transforms **1** to **3** is provided by the isolation and characterization by X-ray crystallography of a stable intermediate, the sodium salt of $[VO(EHGS)]^-$ (**2**), in which EHGS is an abbreviation for *N*-[2-(*o*-salicylideneamino)ethyl](*o*-hydroxyphenyl)glycine. In this complex the vanadyl ion is coordinated by two phenolate oxygen atoms, two nitrogen atoms, and one carboxylate oxygen atom. Crystals of **1** form as light blue blocks in orthorhombic space group $Pna2_1$ with $a = 9.739$ (2) Å, $b = 10.643$ (2) Å, and $c = 22.870$ (8) Å. The measured (1.44 g cm^{-3}) and calculated (1.42 g cm^{-3}) densities are consistent with four molecules of $NH_4[VO(EHPG)] \cdot H_2O \cdot C_2H_5OH$ per unit cell. Orange needles of **2** crystallize in monoclinic space group $P2_1/n$ with $a = 10.939$ (1) Å, $b = 10.517$ (2) Å, $c = 17.261$ (2) Å, and $\beta = 90.428$ (7)°. The measured (1.52 g cm^{-3}) and calculated (1.54 g cm^{-3}) densities indicate four molecules of $Na[VO(EHGS)] \cdot 1.5H_2O \cdot CH_3OH$ per unit cell. Large green blocks of **3** form in monoclinic space group $P2_1/c$ with $a = 14.068$ (2) Å, $b = 12.099$ (1) Å, $c = 17.709$ (2) Å, and $\beta = 100.54$ (1)°. The measured (1.43 g cm^{-3}) and calculated (1.49 g cm^{-3}) densities are in agreement with eight molecules of VO(SALEN) per unit cell. Full-matrix least-squares refinements of the structures have converged with conventional (and weighted) *R* indices (on $|F_o|$) of 0.040 (0.058), 0.040 (0.048), and 0.042 (0.056) for **1**, **2**, and **3**, respectively, with use of (in the same order) 2566, 2913, and 5094 observations of $|F_o|$ with $F_o^2 > 3\sigma(F_o^2)$.

Introduction

As part of a continuing investigation of the mammalian iron transport protein human serum transferrin, studies have been initiated for a number of small molecules as models for the metal ion binding site in this protein.[3-5] This work has centered on metal complexes of ethylenebis[(*o*-hydroxyphenyl)glycine] (EHPG), the Cr^{3+}, Co^{3+}, Cu^{2+}, Mn^{3+}, and Fe^{3+} chelates of which have been isolated and studied.[4,5] Vanadium complexes would be especially interesting in light of the use of this metal as an EPR probe of transferrin,[6] its biological activity,[7] and the suggestion that transferrin may transport and bind this element under conditions of vanadium toxicity.[8] We have found that the chelate chemistry of vanadium in both the +4 and +5 oxidation states with EHPG is quite complex and in the higher oxidation state displays a fascinating metal-assisted, stepwise, oxidative decarboxylation of the ligand, to yield ultimately the previously characterized vanadyl *N,N'*-disalicylideneethylenediamine (SALEN) complex.

In this report we structurally characterize the intermediates in these transformations by examination of the vanadyl complexes of the following: the starting intact ligand, EHPG (this name for the ligand is used for all its protonated and deprotonated forms—the ligand proton stoichiometry in this paper will thus be determined by context); the intermediate, monodecarboxylated monoimine, EHGS; and the final product, SALEN. A brief report of some of this work has already appeared.[9] Detailed chemical analysis of this system is the subject of a companion paper.[10]

Experimental Section

Materials. The ligand EHPG·H_2O ($C_{18}H_{22}N_2O_7$; see Figure 1) was obtained from Sigma Chemical Co. and consisted of an approximately equal mixture of racemic and mesomeric isomers.[4] The material was used without resolution but was purified by Soxhlet extraction with acetone.

Synthesis. The $[NH_4][VO(EHPG)] \cdot H_2O \cdot C_2H_5OH$ (**1**), $Na[VO(EHGS)] \cdot 1.5H_2O \cdot CH_3OH$ (**2**), and VO(SALEN) (**3**) were prepared as described elsewhere.[10] Crystals suitable for X-ray diffraction were obtained by slow evaporation of aqueous ethanol, methanol, or acetone solutions, respectively. Although the preparation and crystallographic characterization of **3** as part of the structure of $([VO(SALEN)]_2Na)BPh_4$ have been reported by others,[11] we have included it here—although not in detail—because it is the stable entity formed upon completion of the stepwise vanadyl-assisted oxidation.

X-ray Crystallography. Data crystals of **1**, **2**, and **3** were obtained from larger specimens by cutting along cleavage planes. The crystals were then affixed to glass fibers with epoxy cement and examined by precession photography. This led to estimates of unit cell parameters and to assignments of probable space groups. Each crystal was then transferred to an Enraf-Nonius CAD-4 diffractometer.[12] Preliminary dif-

* To whom correspondence should be addressed.

(1) University of California.
(2) University of Vermont.
(3) Riley, P. E.; Pecoraro, V. L.; Carrano, C. J.; Raymond, K. N. *Inorg. Chem.* **1983**, *22*, 3096.
(4) Patch, M. G.; Simolo, K. P.; Carrano, C. J. *Inorg. Chem.* **1982**, *21*, 2972.
(5) Patch, M. G.; Simolo, K. P.; Carrano, C. J. *Inorg. Chem.* **1983**, *22*, 2630.
(6) Chasteen, N. D. *Coord. Chem. Rev.* **1977**, *22*, 1.
(7) Josephson, L.; Cantley, L. C. *Biochemistry* **1977**, *16*, 4572.
(8) Harris, W. R.; Friedman, S. B.; Silberman, D. *Inorg. Biochem.* **1984**, *20*, 157.
(9) Pecoraro, V. L.; Bonadies, J. A.; Marrese, C. A.; Carrano, C. J. *J. Am. Chem. Soc.* **1984**, *106*, 3360.
(10) Carrano, C. J.; Bonadies, J. A., submitted for publication.
(11) Pasquali, M.; Marchetti, F.; Floriani, C.; Cesari, M. *Inorg. Chem.* **1980**, *19*, 1198.

0020-1669/86/1325-0154$01.50/0

Table I. Crystallographic Summary[a]

	1	2	3
a, Å	9.739 (2)	10.9387 (9)	14.068 (2)
b, Å	10.643 (2)	10.5173 (25)	12.099 (1)
c, Å	22.870 (8)	17.2609 (15)	17.709 (2)
β, deg		90.428 (7)	100.54 (1)
V, Å^3	2370 (2)	1985.7 (8)	2963 (1)
d_{measd}, g cm^{-3}	1.44[b]	1.52[c]	1.43[d]
d_{calcd}, g cm^{-3}	1.42	1.54	1.49
Z	4	4	8
mol formula	$C_{20}H_{29}N_3O_9V$	$C_{18}H_{23}N_2O_{7.5}NaV$	$C_{16}H_{14}N_2O_3V$
fw	506.14	469.32	332.24
space group	$Pna2_1$ (No. 33)[e]	$P2_1/n$ (No. 14)[f]	$P2_1/c$ (No. 14)
p values	0.04	0.03	0.02
check reflcns	i	i	i
2θ range	3.0–55.0	3.0–55.0	3.0–55.0
no. of total reflcns measd	2866	4485	6783
data cryst dimens, mm	0.33 × 0.57 × 0.62	0.08 × 0.15 × 0.30	0.24 × 0.37 × 0.45
data cryst faces[g]	(011), (0$\bar{1}$1), (01$\bar{1}$)*, (101), (10$\bar{1}$), ($\bar{2}$0$\bar{1}$)*	(001), (00$\bar{1}$), (10$\bar{1}$), ($\bar{1}$01), (1$\bar{1}$1), ($\bar{1}\bar{1}\bar{1}$), (010)*	(010), (0$\bar{1}$0), (100), ($\bar{1}\bar{2}$0), ($\bar{1}$03)*, (10$\bar{3}$)*, ($\bar{4}$0$\bar{1}$)*
abs coeff μ(Mo Kα),[h] cm^{-1}	5.41	5.44	3.63

[a] Unit cell parameters were obtained by least-squares refinement of the setting angles of 24 reflections, formed from subgroups of symmetry-related reflections, with $20 < 2\theta < 23°$, $19 < 2\theta < 24°$, and $24 < 2\theta < 34°$ for **1**–**3**, respectively. Numbers in parentheses are the estimated standard deviations in the least significant digits. [b] Flotation in *n*-hexane/CCl_4. [c] Flotation in CCl_4/bromoform. [d] Flotation in cyclohexane/bromoform. [e] Shown by the final structure (see text). [f] Nonstandard setting of space group $P2_1/c$ with the following general equivalent positions: x, y, z; $\bar{x}, \bar{y}, \bar{z}$; $^1/_2 - x, ^1/_2 + y, ^1/_2 - z$; $^1/_2 + x, ^1/_2 - y, ^1/_2 + z$. [g] Faces marked with an asterisk are not naturally formed but were obtained by cleavage (see text). [h] Examination of reflections with $\chi = 90 \pm 10°$ at approximately regular intervals ($5 < \Delta 2\theta < 10°$) within the 2θ range of data collections by the ψ-scan technique indicated that the normalized transmission factors for all three data crystals were within the range 0.95–1.00; hence, absorption corrections were not applied to these data sets. [i] Small random variation in intensity as a function of time for all three data sets; decay corrections were not necessary.

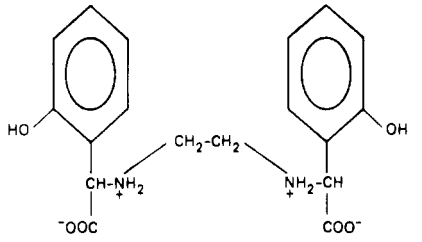

Figure 1. Structural formula of ethylenebis[(*o*-hydroxyphenyl)glycine] (EHPG).

fractometer data confirmed the choices of unit cells and (probable) space groups and also established that each crystal was of high quality, since scans of intense, low-angle reflections showed the peak widths at half-height to be narrow (0.48–0.64° for **1**, 0.54–0.83° for **2**, and 0.51–0.77° for **3**). Following the accurate centering of 24 high-angle reflections from diverse regions of reciprocal space for the data crystals of **1**, **2**, and **3**, intensity data were collected at 22 °C as reported previously.[12] Crystal data and data collection parameters are summarized in Table I. The measured intensities were reduced to structure factor amplitudes and assigned standard deviations (with p values given in Table I) as described earlier.[12] The p factors were chosen to reflect the agreement for averaging of the averaged data.

During the initial data collection, the crystal of **1** deteriorated. In an effort to eliminate or retard this decay a second crystal was cleaved from another large crystal (as before), quickly wedged into a Lindeman capillary tube, and shielded from light during all ensuing experiments. These measures proved effective, since no evidence of degradation was noted with this crystal.

Solution and Refinement of the Structures. The structures of **1**, **2**, and **3** were solved by standard heavy-atom methods and refined by full-matrix least-squares procedures,[12] with only those $|F_o|$ reflections with $F_o^2 > 3\sigma(F_o^2)$ used. Neutral-atom scattering factors for V, Na, O, N, C, and H were used in these calculations and were corrected for the effects of anomalous scattering of Mo K_α radiation.[13]

$[NH_4][VO(EHPG)]\cdot H_2O\cdot C_2H_5OH$ (1). Because the density of the crystals of **1** (see Table I) indicated four formula weights of the salt per unit cell and since the anticipated structure of this complex does not possess either $C_i(\bar{1})$ or $\sigma(m)$ symmetry as required for four formula weight of **1** per unit cell in centrosymmetric space group *Pnma*, the noncentrosymmetric space group $Pna2_1$ was assumed to be correct. This choice was corroborated by the final refinement results in the lower symmetry space group; that is, examination of the atomic fractional coordinates revealed no indication of a mirror plane in the structure.

At least-squares convergence[14] for a model in which nonhydrogen atoms were treated anisotropically, $R = 0.057$, $R_w = 0.078$, and the goodness of fit (GOF) was 4.96.[15] The positions of the ethanol and water molecules were refined isotropically; contributions of the hydrogen atoms were not yet included. Since **1** crystallizes in a noncentrosymmetric space group, the data crystal used in this work was chosen from a racemic mixture of crystals. In an attempt to determine if the proper chirality had been selected during the solution of this structure, the identical refinement of the mirror image structure was carried out and gave $R = 0.052$ and $R_w = 0.071$. The second model corresponds to the correct structure and therefore was used in the remaining calculations. All hydrogen atoms of the EHPG ligand were located from a difference Fourier map with densities of 0.2–0.5 e Å^{-3}. The positions of the hydrogen atoms of the ammonium ion and of the ethanol and water molecules were poorly defined and therefore were not included in the subsequent cycles of refinement. The positions of the EHPG hydrogen atoms were idealized[16] (except for the one bonded to the uncoordinated phenolic oxygen atom, which was maintained at its position from the difference map). Comparison of $|F_o|$ and $|F_c|$ near convergence showed evidence of secondary extinction, so a correction [$2.9\ (8) \times 10^{-7}$ e^{-2}] for this effect was made in the concluding cycles of refinement to give $R = 0.040$, $R_W = 0.058$, and GOF = 2.36 for 2566 observations.[17] In the last cycle of refinement no shift in parameter exceeded 0.43 of a corresponding estimated standard deviation (esd). The largest peaks on a final difference Fourier map were no greater than 0.5 e Å^{-3} and were mainly associated with NH_4^+, H_2O, and C_2H_5OH. For comparison, the carbon atoms of the ethanol molecule, which were subject to appreciable thermal motion, appeared as peaks of 0.7 e Å^{-3} on an earlier difference map. Examination of $|F_o|$ vs. $|F_c|$ as a function of magnitude of $|F_o|$, setting angle, and Miller index showed no significant pattern.

$Na[VO(EHGS)]\cdot 1.5H_2O\cdot CH_3OH$ (2). Full-matrix least-squares convergence was attained for a model in which non-hydrogen atoms were refined anisotropically and hydrogen atoms of the EHGS ligand were

(12) The procedures used for data collection have been described previously: Eigenbrot, C. W., Jr.; Raymond, K. N. *Inorg. Chem.* **1982**, *21*, 2653.
(13) "International Tables for X-Ray Crystallography"; Kynoch Press: Birmingham, England, 1974; Vol. IV.
(14) The function minimized in refinement is $\sum w(|F_o| - |F_c|)^2$, where the weight w is $4F_o^2/\sigma^2(F_o^2)$.
(15) The error indices R and R_w and the standard deviation of an observation of unit weight are defined in ref 12.
(16) The C–H and N–H distances were constrained to 0.95 and 0.87 Å in accordance with a previous study: Churchill, M. R. *Inorg. Chem.* **1973**, *12*, 1213. Hydrogen atoms were assigned fixed thermal parameters of 5.0 (EHGS) and 6.0 (solvate) Å^2 in least-squares refinement.
(17) Zachariasen, W. H. *Acta Crystallogr., Sect A: Cryst. Phys., Diffr., Theor. Gen. Crystallogr.* **1968**, *24*, 212.

Table II. Fractional Coordinates for Non-Hydrogen Atoms of $[NH_4][VO(EHPG)]\cdot H_2O\cdot C_2H_5OH$ (**1**)

atom	*x*	*y*	*z*
V	0.69891 (5)	0.56218 (2)	0.7500 (0)
O(1)	0.7405 (3)	0.4801 (1)	0.7820 (3)
O(2)	0.6630 (3)	0.7694 (1)	0.5540 (3)
O(3)	0.4963 (2)	0.5494 (1)	0.7724 (2)
O(4)	0.8802 (2)	0.5731 (1)	0.6626 (3)
O(5)	0.3037 (2)	0.5128 (1)	0.6944 (3)
O(6)	1.0113 (3)	0.6310 (1)	0.5489 (3)
O(7)	0.7290 (3)	0.5929 (1)	0.8830 (3)
O(8)	0.8463 (3)	0.4629 (2)	0.4128 (4)
O(9)	0.9718 (6)	0.6194 (2)	0.0114 (8)
N(1)	0.6361 (3)	0.5239 (1)	0.5625 (3)
N(2)	0.6562 (3)	0.6396 (1)	0.6421 (3)
N(3)	0.8948 (3)	0.4875 (1)	1.0030 (4)
C(1)	0.4299 (3)	0.5188 (1)	0.6929 (4)
C(2)	0.5168 (4)	0.4873 (1)	0.5952 (4)
C(3)	0.5662 (4)	0.4313 (1)	0.6581 (4)
C(4)	0.6725 (3)	0.4317 (1)	0.7493 (5)
C(5)	0.7099 (4)	0.3789 (2)	0.8069 (5)
C(6)	0.6411 (5)	0.3276 (2)	0.7766 (5)
C(7)	0.5358 (6)	0.3276 (2)	0.6896 (5)
C(8)	0.5002 (5)	0.3791 (2)	0.6305 (5)
C(9)	0.6083 (4)	0.5706 (2)	0.4709 (3)
C(10)	0.5613 (4)	0.6259 (2)	0.5362 (4)
C(11)	0.7884 (3)	0.6664 (1)	0.6009 (3)
C(12)	0.8222 (3)	0.7192 (1)	0.6794 (3)
C(13)	0.9150 (4)	0.7188 (2)	0.7774 (4)
C(14)	0.9368 (5)	0.7686 (2)	0.8481 (4)
C(15)	0.8677 (4)	0.8191 (2)	0.8227 (5)
C(16)	0.7759 (4)	0.8206 (1)	0.7250 (4)
C(17)	0.7525 (4)	0.7711 (1)	0.6521 (4)
C(18)	0.9034 (4)	0.6207 (1)	0.6041 (4)
C(19)	0.9755 (13)	0.6555 (4)	0.1203 (11)
C(20)	0.9074 (16)	0.6293 (7)	0.2220 (12)

Table III. Fractional Coordinates for Non-Hydrogen Atoms of $Na[VO(EHGS)]\cdot 1.5H_2O\cdot CH_3OH$ (**2**)

atom	*x*	*y*	*z*
V	0.15768 (4)	0.09674 (5)	0.23329 (3)
Na	0.1098 (1)	−0.0740 (1)	0.07557 (8)
O(1)	0.2589 (2)	0.0608 (2)	0.1434 (1)
O(2)	0.0911 (2)	−0.0736 (2)	0.2221 (1)
O(3)	0.0236 (2)	0.1464 (2)	0.1358 (1)
O(4)	0.2539 (2)	0.0910 (2)	0.3040 (1)
O(5)	0.0114 (2)	0.2757 (3)	0.0338 (1)
O(6)	−0.1198 (2)	−0.0133 (3)	0.0513 (1)
O(7)	0.2070 (2)	−0.2675 (3)	0.0603 (2)
O(8)	0.0962 (6)	0.4799 (7)	−0.0572 (4)
N(1)	0.1637 (2)	0.2966 (2)	0.2154 (1)
N(2)	0.0099 (2)	0.1476 (2)	0.2993 (1)
C(1)	0.0573 (3)	0.2425 (3)	0.0961 (2)
C(2)	0.1643 (2)	0.3185 (3)	0.1303 (2)
C(3)	0.2846 (2)	0.2749 (3)	0.0961 (2)
C(4)	0.3251 (2)	0.1493 (3)	0.1056 (2)
C(5)	0.4374 (3)	0.1150 (3)	0.0740 (2)
C(6)	0.5073 (3)	0.2008 (3)	0.0343 (2)
C(7)	0.4668 (3)	0.3233 (3)	0.0242 (2)
C(8)	0.3563 (3)	0.3603 (3)	0.0549 (2)
C(9)	0.0571 (3)	0.3590 (3)	0.2535 (2)
C(10)	0.0176 (3)	0.2809 (3)	0.3227 (2)
C(11)	−0.0797 (3)	0.0769 (3)	0.3189 (2)
C(12)	−0.0941 (3)	−0.0545 (3)	0.2980 (2)
C(13)	−0.1996 (3)	−0.1175 (3)	0.3249 (2)
C(14)	−0.2220 (3)	−0.2420 (4)	0.3086 (2)
C(15)	−0.1387 (3)	−0.3102 (3)	0.2649 (2)
C(16)	−0.0341 (3)	−0.2519 (3)	0.2376 (2)
C(17)	−0.0105 (2)	−0.1236 (3)	0.2524 (2)
C(18)	−0.2191 (3)	−0.0745 (4)	0.0874 (2)

fixed at idealized positions.[16] Hydrogen atoms of solvent molecules that were located from a difference Fourier map were maintained at those positions. There was no indication of secondary extinction from an examination of $|F_o|$ vs. $|F_c|$. In the last cycle of refinement, which gave $R = 0.040$, $R_w = 0.048$, and GOF = 1.85 for 2913 observations and 271 variables, no parameter shift exceeded 0.08 of its esd. The largest peaks on a final difference Fourier map were 0.7 e Å^{-3} and were 0.6–0.7 Å from water molecule $H_2O(8)$, which is disordered and of partial occupancy.[18] Examination of $|F_o|$ vs. $|F_c|$ as a function of the magnitude of $|F_o|$, setting angle, and Miller index showed disagreement only for weak, low-angle reflections.

Table IV. Fractional Coordinates for Non-Hydrogen Atoms of VO(SALEN) (**3**)

atom	*x*	*y*	*z*
V(A)	0.10555 (3)	0.42516 (3)	0.41106 (2)
V(B)	0.55170 (3)	0.32421 (4)	0.05357 (3)
O(1A)	−0.0146 (1)	0.4157 (1)	0.33959 (9)
O(2A)	0.0522 (1)	0.3139 (1)	0.46865 (9)
O(3A)	0.1942 (1)	0.3717 (1)	0.37998 (10)
O(1B)	0.5853 (1)	0.4204 (2)	0.14092 (12)
O(2B)	0.6526 (1)	0.3936 (2)	0.01023 (11)
O(3B)	0.5845 (2)	0.2008 (2)	0.07446 (15)
N(1A)	0.1119 (1)	0.5869 (2)	0.3787 (1)
N(2A)	0.1595 (2)	0.4998 (2)	0.5142 (1)
N(1B)	0.4119 (1)	0.3299 (2)	0.0724 (1)
N(2B)	0.4736 (2)	0.3193 (2)	−0.0566 (1)
C(1A)	−0.0049 (2)	0.5762 (2)	0.2612 (1)
C(2A)	−0.0461 (2)	0.4746 (2)	0.2767 (1)
C(3A)	−0.1269 (2)	0.4360 (2)	0.2250 (1)
C(4A)	−0.1613 (2)	0.4923 (2)	0.1581 (1)
C(5A)	−0.1179 (2)	0.5888 (2)	0.1406 (1)
C(6A)	−0.0420 (2)	0.6318 (2)	0.1918 (1)
C(7A)	0.0676 (2)	0.6298 (2)	0.3163 (1)
C(8A)	0.1844 (2)	0.6509 (2)	0.4311 (2)
C(9A)	0.1809 (2)	0.6183 (2)	0.5107 (2)
C(10A)	0.1719 (2)	0.4521 (2)	0.5804 (1)
C(11A)	0.1441 (2)	0.3427 (2)	0.5952 (1)
C(12A)	0.0839 (2)	0.2779 (2)	0.5392 (1)
C(13A)	0.0534 (2)	0.1745 (2)	0.5603 (1)
C(14A)	0.0813 (2)	0.1342 (2)	0.6334 (2)
C(15A)	0.1414 (2)	0.1958 (3)	0.6888 (1)
C(16A)	0.1719 (2)	0.2990 (2)	0.6700 (1)
C(1B)	0.4448 (2)	0.4060 (2)	0.1998 (2)
C(2B)	0.5423 (2)	0.4349 (2)	0.2003 (2)
C(3B)	0.5945 (3)	0.4837 (3)	0.2673 (2)
C(4B)	0.5535 (3)	0.5023 (4)	0.3298 (2)
C(5B)	0.4589 (3)	0.4729 (4)	0.3302 (2)
C(6B)	0.4054 (3)	0.4273 (3)	0.2670 (2)
C(7B)	0.3839 (2)	0.3615 (2)	0.1332 (2)
C(8B)	0.3421 (2)	0.2847 (4)	0.0081 (2)
C(9B)	0.3668 (2)	0.3187 (3)	−0.0641 (2)
C(10B)	0.5101 (2)	0.3153 (3)	−0.1177 (2)
C(11B)	0.6096 (2)	0.3306 (2)	−0.1204 (2)
C(12B)	0.6754 (2)	0.3718 (2)	−0.0579 (2)
C(13B)	0.7693 (2)	0.3937 (3)	−0.0691 (2)
C(14B)	0.7962 (2)	0.3729 (3)	−0.1389 (2)
C(15B)	0.7317 (3)	0.3301 (3)	−0.1997 (2)
C(16B)	0.6402 (3)	0.3117 (3)	−0.1908 (2)

VO(SALEN) (3). As noted above, the crystal structure of this complex, in a different form, has been reported earlier.[11] Refinement of this structure gave $R = 0.042$, $R_w = 0.056$, and GOF = 3.13 for 5094 observations and 397 variables. The largest shift in a parameter in the final cycle of refinement was 0.64 of a corresponding esd. There was no evidence of secondary extinction. The largest peaks on a final difference Fourier map were 0.2–0.4 e Å^{-3}, many of which were associated with the ethylenediamine moieties (two per asymmetric unit; see Table I), which are slightly disordered. Carbon atoms of an earlier difference map exhibited peaks of 1.7–3.8 e Å^{-3}. Examination of $|F_o|$ vs. $|F_c|$ at the end of refinement showed disagreement for the very weak reflections but no trend as a function of setting angle or Miller index.

Tables II–IV present atomic positional parameters of the structures of **1–3**, with esd's as derived from the inverse matrix at final refinement. Listings of anisotropic thermal parameters for **1–3** (Tables V–VII), hydrogen atom parameters for **1–3** (Tables VIII–X), and observed and calculated structure factor amplitudes for **1–3** (Tables XI–XIII) are available.[19]

Discussion

Figures 2–4 are drawings of the VO complexes reported in this paper and indicate the atom-numbering schemes employed herein. Listings of bond lengths and bond angles for **1–3** are given in Tables XIV–XVI, respectively.

(18) Analytical data for **2** is given in ref 10.
(19) See paragraph at end of paper regarding supplementary material.

Table XIV. Bond Lengths (Å) and Angles (deg) for $[VO(EHPG)]^-$ (**1**)[a]

V–O(1)	1.950 (2)	N(1)–C(2)	1.473 (3)
V–O(3)	2.009 (2)	N(1)–C(9)	1.472 (3)
V–O(4)	2.011 (2)	N(2)–C(10)	1.492 (3)
V–O(7)	1.607 (2)	N(2)–C(11)	1.491 (3)
V–N(1)	2.264 (2)	C(1)–C(2)	1.523 (4)
V–N(2)	2.152 (2)	C(2)–C(3)	1.524 (3)
O(1)–C(4)	1.335 (3)	C(9)–C(10)	1.513 (4)
O(2)–C(17)	1.360 (3)	C(11)–C(12)	1.506 (3)
O(3)–C(1)	1.274 (3)	C(11)–C(18)	1.532 (3)
O(4)–C(18)	1.274 (3)	mean phenyl C–C[b]	1.387 (4)
O(5)–C(1)	1.236 (3)		
O(6)–C(18)	1.227 (3)		

V–O(1)–C(4)	130.4 (2)	C(2)–C(3)–C(4)	121.6 (2)
V–O(3)–C(1)	120.0 (2)	C(2)–C(3)–C(8)	119.0 (2)
V–O(4)–C(18)	119.2 (2)	O(1)–C(4)–C(3)	123.1 (2)
V–N(1)–C(2)	103.0 (2)	O(1)–C(4)–C(5)	118.1 (3)
V–N(1)–C(9)	110.6 (1)	N(1)–C(9)–C(10)	111.0 (2)
C(2)–N(1)–C(9)	115.0 (2)	C(9)–C(10)–N(2)	109.6 (2)
V–N(2)–C(10)	110.4 (1)	N(2)–C(11)–C(12)	110.7 (2)
V–N(2)–C(11)	109.1 (1)	N(2)–C(11)–C(18)	110.2 (2)
C(10)–N(2)–C(11)	113.5 (2)	C(12)–C(11)–C(18)	112.0 (2)
O(3)–C(1)–O(5)	123.8 (2)	C(11)–C(12)–C(13)	123.9 (2)
O(3)–C(1)–C(2)	115.6 (2)	C(11)–C(12)–C(17)	117.4 (2)
O(5)–C(1)–C(2)	120.6 (2)	O(2)–C(17)–C(12)	116.6 (2)
C(1)–C(2)–C(3)	105.9 (2)	O(2)–C(17)–C(16)	123.7 (2)
C(1)–C(2)–N(1)	109.3 (2)	O(4)–C(18)–O(6)	123.3 (2)
C(3)–C(2)–N(1)	109.4 (2)	C(11)–C(18)–O(4)	117.6 (2)
		C(11)–C(18)–O(6)	119.0 (2)

[a] Numbers in parentheses are the estimated standard deviations in the least significant digits. See Figure 2 for identity of the atoms. [b] A mean bond length is given by $\bar{l} = \sum_i^n l_i/n$ and its standard deviation by $\sigma(\bar{l}) = [\sum(l_i - \bar{l})^2/n(n-1)]^{1/2}$.

Table XV. Bond Lengths (Å) and Angles (deg) for $[VO(EHGS)]^-$ (**2**)[a]

V–O(1)	1.949 (1)	N(1)–C(2)	1.487 (3)
V–O(2)	1.943 (1)	N(1)–C(9)	1.495 (3)
V–O(3)	2.285 (1)	N(2)–C(10)	1.462 (3)
V–O(4)	1.606 (1)	N(2)–C(11)	1.278 (3)
V–N(1)	2.126 (2)	C(1)–C(2)	1.531 (3)
V–N(2)	2.055 (2)	C(2)–C(3)	1.518 (3)
O(1)–C(4)	1.351 (2)	C(9)–C(10)	1.515 (3)
O(2)–C(17)	1.339 (2)	C(11)–C(12)	1.437 (3)
O(3)–C(1)	1.277 (3)	mean phenyl C–C[b]	1.39 (2)
O(5)–C(1)	1.234 (3)		

V–O(1)–C(4)	124.1 (1)	O(1)–C(4)–C(5)	119.2 (2)
V–O(2)–C(17)	129.4 (1)	O(2)–C(17)–C(12)	123.9 (2)
V–O(3)–C(1)	112.6 (1)	O(2)–C(17)–C(16)	117.4 (2)
V–N(1)–C(2)	107.1 (1)	O(3)–C(1)–C(2)	115.4 (2)
V–N(1)–C(9)	110.2 (1)	O(3)–C(1)–O(5)	125.0 (2)
V–N(2)–C(10)	111.1 (1)	C(2)–C(1)–O(5)	119.5 (2)
V–N(2)–C(11)	127.2 (1)	C(3)–C(4)–C(5)	118.4 (2)
C(4)–C(3)–C(2)	120.9 (2)	C(4)–C(5)–C(6)	121.4 (2)
C(8)–C(3)–C(2)	119.8 (2)	C(5)–C(6)–C(7)	120.1 (2)
C(3)–C(2)–N(1)	110.4 (2)	C(6)–C(7)–C(8)	119.9 (2)
C(2)–N(1)–C(9)	112.0 (2)	C(7)–C(8)–C(3)	120.9 (2)
N(1)–C(9)–C(10)	109.7 (2)	C(8)–C(3)–C(4)	119.3 (2)
C(9)–C(10)–N(2)	108.6 (2)	C(12)–C(13)–C(14)	122.0 (2)
C(10)–N(2)–C(11)	121.8 (2)	C(13)–C(14)–C(15)	119.4 (2)
N(2)–C(11)–C(12)	125.2 (2)	C(14)–C(15)–C(16)	120.3 (2)
C(11)–C(12)–C(13)	117.2 (2)	C(15)–C(16)–C(17)	121.2 (2)
C(11)–C(12)–C(17)	124.4 (2)	C(16)–C(17)–C(12)	118.6 (2)
O(1)–C(4)—C(3)	122.4 (2)	C(17)–C(12)–C(13)	118.4 (2)

[a] Numbers in parentheses are the estimated standard deviations in the least significant digits. See Figure 3 for identity of the atoms. [b] The mean bond length and its standard deviation were determined with the expressions given in the caption of Table XIV.

The crystal structure of **1** consists of NH_4^+ ions that are hydrogen bonded directly to uncoordinated carboxylate oxygen atoms, O(5) and O(6), and indirectly through water molecules, $H_2O(8)$, to ethanol oxygen atoms O(9). This arrangement is shown in Figure 5 and summarized in Table XVII.[19]

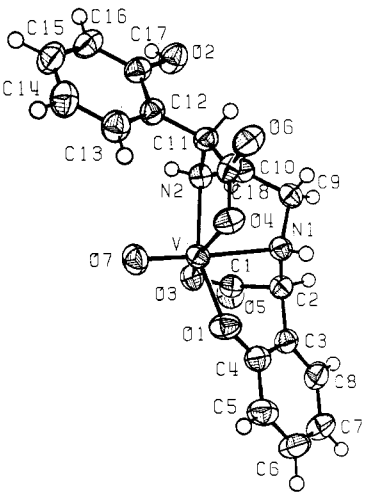

Figure 2. Perspective view of the $[VO(EHPG)]^-$ ion in **1**. Non-hydrogen atoms are drawn as ellipsoids of 50% probability, and hydrogen atoms as spheres of radius 0.1 Å.

Table XVI. Bond Lengths (Å) and Angles (deg) for VO(SALEN) (**3**)[a]

	molecule A	molecule B
V–O(1)	1.921 (1)	1.924 (1)
V–O(2)	1.922 (1)	1.925 (1)
V–O(3)	1.590 (1)	1.587 (1)
V–N(1)	2.046 (1)	2.055 (1)
V–N(2)	2.054 (1)	2.057 (1)
O(1)–C(2)	1.328 (2)	1.318 (2)
O(2)–C(12)	1.320 (2)	1.330 (2)
N(1)–C(7)	1.276 (2)	1.271 (2)
N(1)–C(8)	1.467 (2)	1.467 (2)
N(2)–C(9)	1.469 (2)	1.485 (2)
N(2)–C(10)	1.290 (2)	1.281 (2)
C(1)–C(7)	1.431 (2)	1.430 (3)
C(8)–C(9)	1.472 (3)	1.445 (3)
C(10)–C(11)	1.418 (2)	1.421 (2)
mean phenyl C–C[b]	1.393 (5)	1.386 (8)
O(1)–V–O(2)	85.76 (4)	88.07 (5)
O(1)–V–O(3)	113.51 (5)	111.33 (7)
O(1)–V–N(1)	87.18 (4)	87.17 (5)
O(1)–V–N(2)	138.54 (5)	142.16 (6)
O(2)–V–O(3)	107.80 (5)	107.40 (7)
O(2)–V–N(1)	149.29 (5)	147.91 (6)
O(2)–V–N(2)	87.30 (5)	86.51 (5)
O(3)–V–N(1)	102.43 (5)	103.88 (7)
O(3)–V–N(2)	107.53 (5)	106.02 (8)
N(1)–V–N(2)	78.48 (5)	78.12 (6)
V–O(1)–C(2)	129.73 (8)	129.89 (10)
V–O(2)–C(12)	129.47 (9)	126.38 (11)
V–N(1)–C(7)	126.3 (1)	127.0 (1)
V–N(1)–C(8)	112.3 (1)	112.8 (1)
V–N(2)–C(9)	115.9 (1)	116.2 (1)
V–N(2)–C(10)	125.3 (1)	125.1 (1)
O(1)–C(2)–C(1)	123.1 (1)	123.2 (2)
C(2)–C(1)–C(7)	122.1 (1)	122.2 (2)
C(7)–N(1)–C(8)	120.4 (1)	120.1 (2)
N(1)–C(8)–C(9)	108.8 (1)	110.2 (2)
C(8)–C(9)–N(2)	110.2 (1)	109.0 (2)
C(9)–N(2)–C(10)	118.7 (1)	118.7 (2)
N(2)–C(10)–C(11)	126.1 (1)	125.0 (2)
C(10)–C(11)–C(12)	122.4 (1)	122.2 (2)
C(11)–C(12)–O(2)	122.3 (1)	123.6 (2)

[a] Numbers in parentheses are the estimated standard deviations in the least significant digits. See Figure 4 for identity of the atoms. [b] The mean C–C bond length and its corresponding esd are defined in the caption of Table XIV.

As shown in Figure 2, VO^{2+} is bonded to five atoms of the $[EHPG]^{3-}$ ligand, thereby forming a pseudooctahedron about V^{4+}. The most distinguishing aspect of this structure is that vanadyl oxygen atom O(7) is trans (174°) to N(1). In every previously

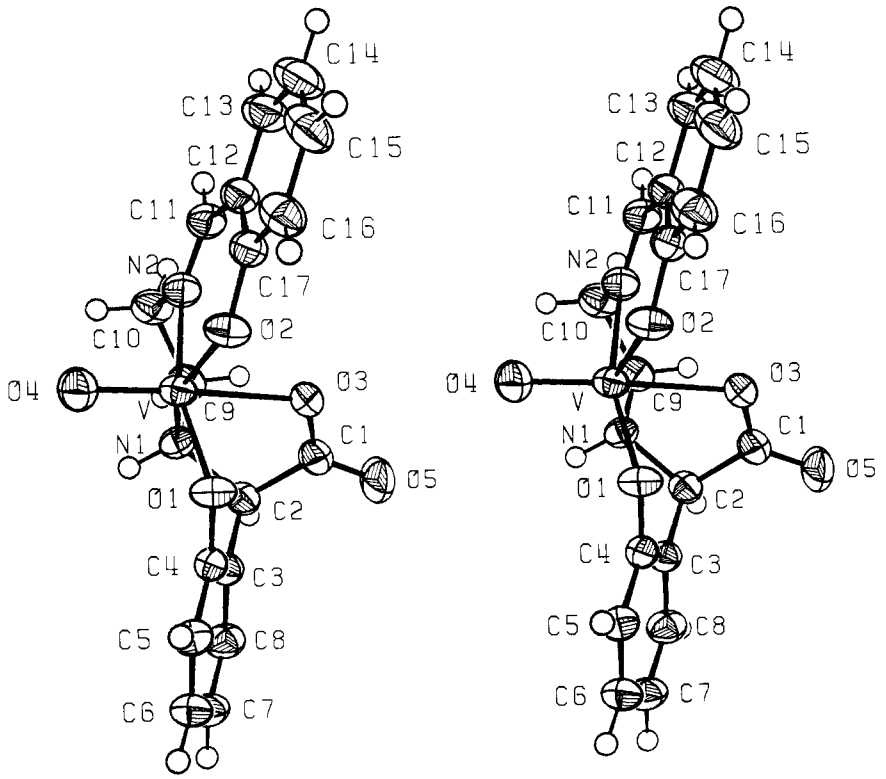

Figure 3. Stereoscopic view of the $[VO(EHGS)]^-$ ion in **2** indicating the atom-numbering scheme. Non-hydrogen atoms are drawn as ellipsoids of 30% probability; hydrogen atoms are shown as spheres of 0.1 Å radius.

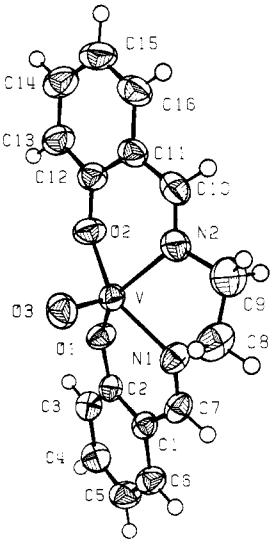

Figure 4. Perspective view of VO(SALEN) (**3**) indicating the atom-numbering scheme. Non-hydrogen atoms are shown as ellipsoids of 50% probability, and hydrogen atoms as spheres of radius 0.1 Å.

structurally characterized metallo EHPG complex, the two amine nitrogens lie within the equatorial plane of the metal coordination sphere. To accommodate this geometry, phenolate atom O(2) is not coordinated in this complex and remains protonated. This is not surprising as the pH of the solution from which the crystal arose was between 3 and 5. We believe that this conformation is stable only under acidic conditions. As the pH is raised, the phenolate oxygen affinity for VO^{2+} increases, resulting in the displacement of a carboxylate moiety in favor of the phenolate. Alternatively, the fact that a nitrogen atom [N(1)] is trans to vanadyl oxygen atom O(7) rather than an oxygen atom may be a consequence of chelate ring strain in this complex. That is, because of the pronounced deviation of V^{4+} from the four-atom plane that is approximately normal to the V-O(7) bond (see Table XVIII[19]), a six-membered ring—of which there is only one in this complex—in this orientation, rather than a five-membered ring, more satisfactorily completes the coordination sphere of the metal. Some support for this suggestion is obtained from the structure of $[VO(EHGS)]^-$ in which the bound carboxylate atom O(3), which is part of a five-membered ring, is trans to vanadyl oxygen atom O(4). In this complex, the angle formed at V^{4+} by the VO ion and the trans oxygen atom is 169°, while the corresponding angle in **1** [O(4)–V–N(1)] is a more relaxed 174°, consistent with a reduction in ring strain as the chelate ring increases from five to six atoms. Moreover, the greater length (by 0.11 Å) of the V–N(1) bond, which is trans to the VO group, compared to that of the V–N(2) bond (which is cis to VO) is due to the strong preference of the VO group for square-pyramidal coordination,[21] with the bond from the donor atom of a more flexible six-membered ring being longer at this trans position.

As established in our earlier study[3] of the Co^{3+}, Ga^{3+}, and Cu^{2+} complexes of EHPG, the configuration of the chiral carbon atoms in this ligand dictate which geometrical isomers form upon metal complexation. In particular, with the racemic form of the ligand (i.e., the isomer with the same chirality at the two asymmetric carbon atoms), the isomer in which the carboxylate oxygen atoms are trans to the four-atom plane containing the two nitrogen atoms has been found from an examination of CPK models to be the most stable. In fact, this is the only mode of octahedral coordination of the racemic isomer that has been found in the crystalline state.[3,20]

The crystal structure of **2** is composed of a network of Na^+ and $[VO(EHGS)]^-$ ions and methanol and water molecules that are linked via hydrogen bonds (see Table XIX[19]). The Na^+ ions are coordinated with three EHGS oxygen atoms, one water molecule, and one methanol molecule in an irregular manner, with bond lengths of 2.32–2.72 Å. Although the position of water molecule $H_2O(8)$ is partially occupied (~0.5), it forms hydrogen bonds to the EHGS ligand and to symmetry-related $H_2O(8)$ molecules. The coordination sphere of the V^{4+} ion is octahedral, with oxygen atom O(5) of the carboxylate group occupying the position trans to the vanadyl oxygen atom and with the two nitrogen atoms and

(20) Bailey, N. A.; Cummins, D.; McKenzie, E. D.; Worthington, J. N. *Inorg. Chim. Acta* **1981**, *50*, 111.
(21) Cotton, F. A.; Wilkinson, G. "Advanced Inorganic Chemistry, A Comprehensive Text", 4th ed.; Wiley: New York, 1980; pp 714–716.

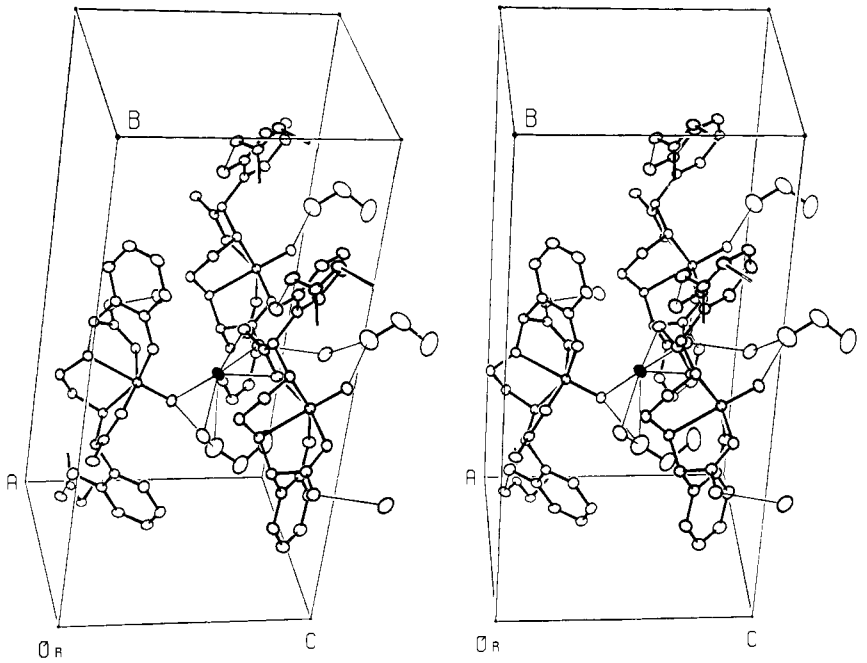

Figure 5. Packing environment about NH_4^+ (darkened ellipsoid) in **1**. Hydrogen bonds are drawn as thin lines. Non-hydrogen atoms are shown as ellipsoids of 15% probability. Hydrogen atoms have been omitted for clarity.

the phenolate oxygen atoms residing at equatorial positions about the metal. Because of the length of the $N-(CH_2)_2-N$ bridge, the nitrogen and the phenolate atoms are mutually cis. As a result of the first step of the VO-assisted oxidative decarboxylation of the EHPG ligand and the strength of the $V{=}O^{2+}$ bond, the geometry about the vanadium ion is particularly irregular. Thus, due to the strong preference of the VO^{2+} group for square-pyramidal coordination, the V–O(carboxylate) bond [i.e. V–O(3)] is ca. 0.3 Å longer than in the octahedral $[VO(EHPG)]^-$ complex (where the carboxylate groups are cis to the VO group). Also, as a consequence of the change in hybridization at the imino nitrogen atom [N(2)], the two V–N bonds differ by ca. 0.07 Å, with the V–N(2) (imino) distance equivalent to the two V–N(imino) distances in VO(SALEN). This change in hybridization from sp^3 to sp^2 is also reflected in the bond angles at N(2) [111, 122, and 127° compared to 107–112° at N(1)].

The crystal structure of **3** is formed by discrete molecules of VO(SALEN) with no unusual intermolecular contacts. The molecules exhibit square-pyramidal coordination in which the imino nitrogen atoms and the phenolate oxygen atoms are, as a result of chelate ring size, mutually cis. As shown in Table XVIII,[19] the deviation of the vanadium ion from the four-atom coordination plane, which is approximately normal to the VO bonds, is 0.13–0.14 Å greater in this five-coordinate complex than in the two six-coordinate complexes **1** and **2**. In general, all aspects of the structures of the two independent molecules per unit cell (see Experimental Section) are in agreement with those reported earlier for $([VO(SALEN)]_2Na)BPh_4$.[11]

The well-established, strong correlations between changes in V=O stretching frequency in the IR region and changes in V=O bond length are apparent from an examination of Table XX. For example, the small increase in V=O distance (0.02 Å) from that in five-coordinate VO(SALEN) to that in six-coordinate $[VO(EHPG)]^-$ is accompanied by a large increase in V=O stretching frequency (ca. 30 cm^{-1}). This correlation is even greater between the V—O(ligand) bond length and $\nu_{V=O}$. Of course, multiple bond lengths are usually less sensitive to bond order changes than single bonds. These effects are seen in Table XX. There is a corresponding lengthening of both the V=O and V—O(ligand) bonds as $\nu_{V=O}$ decreases from 981 cm^{-1} in VO(SALEN) to 921 cm^{-1} in $VO(catechol)_2$,[22] indicating greater electron donation to the metal center. In the case of $VO(EHPG)^-$ and $VO(EHGS)^-$ the donation is from an amine or carboxylate donor trans to the V=O group. The catechol group which is cis to V=O is an inherently better electron donor than the simple phenols of the other complexes.

Table XX. Correlation between VO Stretching Frequency ν (cm^{-1}) and VO Bond Lengths (Å)[a]

complex[b]	ν	V=O	V—O	ref
$VO(cat)_2$	921	1.616	1.956	22
$VO(EHPG)^-$ (**1**)	948	1.607	1.950	this work
$VO(EHGS)^-$ (**2**)	952	1.606	1.946	this work
VO(SALEN) (**3**)	981	1.588	1.922	this work, 23

[a] Spectra were recorded as KBr disks with a Perkin-Elmer 597 spectrophotometer. [b] For ligand abbreviations see text.

We have observed that a DMF solution of VO(EHPG) will oxidatively decarboxylate to generate VO(SALEN).[9,10] In methanol, an intermediate VO(EHGS) species can be isolated, indicating that the process occurs in a stepwise manner. Our initial interest in this system was to establish structural parameters for the reactive species of this conversion. Many attempts at crystallization of **1** and **2** in their reactive V^{5+} forms failed due to their pronounced instability. However, we have succeeded in structurally characterizing the various ligand forms as stable vanadyl complexes. These VO^{2+} species are stable in aqueous solutions but are readily oxidized by molecular oxygen in less polar solvents to the reactive VO^{3+} forms.

In light of the completely reversible electrochemical oxidation of **2** to its vanadium(V) analogue, no substantial structural changes are expected to accompany this redox change. Thus, the vanadyl complex reported here is probably a good model for the reactive species. This is significant because the carboxyl group must be coordinated in the reactive vanadium(V) form of **2** in the same manner as it is in the vanadyl(IV) complex reported here (**2**). The vanadium(V) complex is very rapidly decarboxylated to **3** in DMF under mild conditions, this suggests that the reaction must be *intra*molecular rather than *inter*molecular. Thus, it is the coordinated carboxyl group that is lost upon decarboxylation. Further

(22) Cooper, S. R.; Koh, Y. B.; Raymond, K. N. *J. Am. Chem. Soc.* **1982**, *104*, 5092.

(23) In the VO(SALEN) structure reported in ref 11, the VO moieties are coordinated with Na^+ ions. This weakens the V=O interaction. Hence, the V=O stretching frequency there is reduced by ~20 cm^{-1} to 960 cm^{-1}.

work on elucidating the mechanism of this remarkable transformation is in progress.

In contrast to **2**, the $VO(EHPG)^-$ structure presented herein may not represent the vanadyl analogue of the reactive V^{5+} species. The existence of this compound requires an acidic medium to protonate a phenolate moiety. In DMF, we would expect that the phenol is directly associated with the V^{5+} ion and that the uncoordinated arm is the carboxylate moiety, which is not subject to the first oxidative decarboxylation. Further details of this chemical transformation are reported elsewhere.[10]

Summary

We report the structures of a series of vanadyl complexes that are associated with a novel stepwise oxidative decarboxylation of VO(EHPG) to VO(SALEN). Isolation of the $VO(EHGS)^-$ complex, a structural analogue of the reactive VO(EHGS) intermediate, demonstrates that the carboxylate moiety is directly coordinated to metal, and this in turn supports an intramolecular mechanism for the decarboxylation pathway. That VO(SALEN) is the final product of the reaction scheme is proven by crystal structure analysis.

Acknowledgment. This research was supported by NIH Grant HL 24775 (now Grant AM-32999).

Registry No. 1, 99016-50-9; **2**, 89890-30-2; **3**, 36913-44-7.

Supplementary Material Available: Table V [anisotropic thermal parameters for $[NH_4][VO(EHPG)]\cdot H_2O\cdot C_2H_5OH$], Table VI [anisotropic thermal parameters for $Na[VO(EHGS)]\cdot 1.5H_2O\cdot CH_3OH$], Table VII [anisotropic thermal parameters for VO(SALEN)], Table VIII [hydrogen atom parameters for $[NH_4][VO(EHPG)]\cdot H_2O\cdot C_2H_5OH$], Table IX [hydrogen atom parameters for $Na[VO(EHGS)]\cdot 1.5H_2O\cdot CH_3OH$], Table X [hydrogen atom parameters for VO(SALEN)], Table XI [structure factor amplitudes for $[NH_4][VO(EHPG)]\cdot H_2O\cdot C_2H_5OH$], Table XII [structure factor amplitudes for $Na[VO(EHGS)]\cdot 1.5H_2O\cdot CH_3CH_3OH$], Table XIII [structure factor amplitudes for VO(SALEN)], Table XVII [selected intermolecular distances (Å) for $[NH_4][VO(EHPG)]\cdot H_2O\cdot C_2H_5OH$], Table XVIII [selected mean planes in **1**-**3**], and Table XIX [selected intermolecular distances (Å) for $Na[VO(EHGS)]\cdot 1.5H_2O\cdot CH_3OH$] (63 pages). Ordering information is given on any current masthead page.

Contribution from the School of Chemical Sciences, University of Illinois, Urbana, Illinois 61801

Dynamics of Spin-State Interconversion and Cooperativity for Ferric Spin-Crossover Complexes in the Solid State. 6.[1] Magnetic and Spectroscopic Characterizations of $[Fe(3\text{-}OEt\text{-}SalAPA)_2]X$ ($X = ClO_4^-$, BPh_4^-)

Mark D. Timken, A. M. Abdel-Mawgoud, and David N. Hendrickson*

Received May 21, 1985

The spin-crossover transformation is examined for two ferric complexes of the composition $[Fe(3\text{-}OEt\text{-}SalAPA)_2]X$, where X is either ClO_4^- or BPh_4^- and 3-OEt-SalAPA is the monoanionic Schiff base derived from 3-ethoxysalicylaldehyde and *N*-(3-aminopropyl)aziridine. Variable-temperature magnetic susceptibility, EPR, and Mössbauer data are analyzed for these two complexes. Both are seen to undergo spin-crossover transformations that are more gradual than that observed for the benzene solvate of the $X = ClO_4^-$ compound, which was studied in the previous paper in this series. EPR spectra of the two complexes in this study show that both have d_{xy} low-spin ground states. More importantly, it is found that the two complexes interconvert slower than the EPR time scale but faster than the ^{57}Fe Mössbauer time scale. This shows that neither desolvating the $X = ClO_4^-$ benzene solvate nor replacing the ClO_4^- anion by the BPh_4^- counterion measurably reduces the rate of spin flipping of the $[Fe(3\text{-}OEt\text{-}SalAPA)_2]^+$ cation.

Introduction

The study of solid-state spin-crossover transformations affords a means for examining the coupling of an intramolecular process, the high-spin $\rightleftharpoons$ low-spin interconversion, to the intermolecular interactions inherent to the solid state. In the ferric case, the spin-crossover event involves an intramolecular transfer of the two electrons between the t_{2g}-type and e_g-type d orbitals. Due to the antibonding character of the e_g orbitals, significant metal-ligand bond length changes accompany the spin-state interconversion process. The solid must be able to accommodate these coordination sphere contractions and expansions if molecules of both spin states are to reside within the *same* lattice. Although it has been shown[2] that thermally discontinuous spin-crossover transformations are accompanied by discontinuous lattice changes, it has also been demonstrated[1,3,4] that dramatic lattice rearrangements do not usually accompany thermally gradual transformations. Instead, the lattice parameters show gradual temperature-dependent changes. Recent efforts in spin-crossover research have centered to a large extent on determining the factors that influence the *bulk* properties of the solid-state transformation. It is important, as well, to gain some understanding of the means by which intermolecular interactions inhibit or enhance the *rates* of intramolecular spin-state interconversions.

These solid-state rates have typically been estimated relative to the time scales associated with various spectroscopic techniques (e.g., for Mössbauer $\tau \approx 10^{-7}$ s and for EPR $\tau \approx 10^{-10}$ s). Until recently, only the ferric dithiocarbamates,[5] monothiocarbamates,[6] and diselenocarbamates[7] have been shown to interconvert spin states rapidly on the Mössbauer time scale. Within the past few years, however, a number of ferric complexes with N_4O_2 ligand atom donor sets have also been shown[1,8-13] to interconvert rapidly

(1) Part 5: Timken, M. D.; Strouse, C. E.; Soltis, S. M.; Daverio, S.; Hendrickson, D. N.; Abdel-Mawgoud, A. M.; Wilson, S. R. *J. Am. Chem. Soc.*, in press.
(2) König, E.; Ritter, G.; Irler, W.; Goodwin, H. A. *J. Am. Chem. Soc.* **1980**, *102*, 4681.
(3) König, E.; Ritter, G.; Kulsbreshtha, S. K.; Nelson, S. M. *J. Am. Chem. Soc.* **1983**, *105*, 1924.
(4) (a) Albertsson, J.; Oskarsson, A. *Acta Crystallogr. Sect. B: Struct. Crystallogr. Cryst. Chem.* **1977**, *B33*, 1871. (b) Albertsson, J.; Oskarsson, A.; Stahl, K.; Svenson, C.; Ymen, I. *Acta Crystallogr. Sect. B: Struct. Crystallogr. Cryst. Chem.* **1981**, *B37*, 50.
(5) Merrithew, P. B.; Rasmussen, P. G. *Inorg. Chem.* **1972**, *11*, 325.
(6) Kunze, K. R.; Perry, D. L.; Wilson, L. J. *Inorg. Chem.* **1977**, *16*, 594.
(7) DeFilipo, D.; Depalano, P.; Diaz, A.; Steffe, S.; Trogu, E. F. *J. Chem. Soc., Dalton Trans.* **1977**, 1566.
(8) Maeda, Y.; Tsutsumi, N.; Takashima, Y. *Chem. Phys. Lett.* **1982**, *88*, 248.
(9) Maeda, Y.; Ohshio, H.; Takashima, Y. *Chem. Lett.* **1982**, 943.
(10) Ohshio, H.; Maeda, Y.; Takashima, Y. *Inorg. Chem.* **1983**, *22*, 2684.
(11) Maeda, Y.; Tsutsumi, N.; Takashima, Y. *Inorg. Chem.* **1984**, *23*, 2440.
(12) Federer, W. D.; Hendrickson, D. N. *Inorg. Chem.* **1984**, *23*, 3861.

0020-1669/86/1325-0160$01.50/0